

SLAC-PUB-5577  
June 1991  
(T)

# Dressed Skeleton Expansion in 1 + 1 Dimensional Field Theory Models\*

HUNG JUNG LU

*Stanford Linear Accelerator Center*

*Stanford University*

*Stanford, California 94309*

## ABSTRACT

We discuss the implementation of the Dressed Skeleton Expansion (DSE) and analyse various features of this perturbative calculational method in simple field theory models in 1 + 1 dimension. In particular, we investigate issues concerning loop skeleton diagrams, renormalization in the massive case, and the usage of DSE for vertices involving matrix structures.

*Submitted to Physical Review D*

---

\* Work supported by the Department of Energy, contract DE-AC03-76SF00515.

In a previous paper,<sup>1</sup> we have pointed out that the Dressed Skeleton Expansion (DSE) offers a calculational method in perturbative quantum field theories without scale ambiguity problem. In particular, we illustrated the usage of the method for  $\phi^3$  theory in six dimensions. The basic motivation in choosing this theory resides in its resemblance with Quantum Chromodynamics (QCD) in the aspects of both being renormalizable theories and presenting asymptotic freedom. However, the high dimensionality of the theory hampered the discussion of higher order skeleton graphs.

In this paper we study the application of the DSE to field theories models in  $1 + 1$  dimension. Our purpose is to analyse and discuss the various features and technical details for the implementation of the DSE method, by using simple models as testground. It is not our goal to obtain new results in these simple field theory models, for there exists abundant literature on the subject.<sup>2,3</sup>

This paper is organized in the following five sections.

In section I, we review briefly the general scale setting problem in quantum field theories, and present the DSE as a scale-ambiguity-free calculational method.

In section II we apply the DSE method to massless Gross-Neveu model in leading  $1/N$  expansion, and show that DSE leads to exact four-fermion vertex function, no matter whether we choose to dress up the charged two-point function or the three-point function.

In section III we apply the DSE method to the massless Thirring model. Here we offer an explicit example of a non-trivial loop skeleton diagram, showing that it indeed can be done and yields a finite result, despite the singularity of the

coupling vertex at the Landau pole. We give an argument for the insensitivity of loop skeleton diagrams to the infrared behavior of vertex functions.

In section IV we apply the DSE method to the super-renormalizable massive Yukawa model in 1+1 dimension. This is an example where the vertex function has a non-trivial matrix structure, and special attention is required to select a coupling function that assures continuity of the off-shell to on-shell transition. Also, in this example, we show how to isolate the mass renormalization from particle propagators and absorb all renormalization effects of two-point functions into effective wavefunction renormalization constants.

Finally, in section V, we make some comments and summarize the main conclusions.

## I. Scale Setting Problem and the Dressed Skeleton Expansion

Much of the material in this section has been exposed in ref. 1. However, we have included this section here to complete our presentation.

Perturbative calculations in quantum field theories are usually expressed as power series in a fixed coupling constant. At high transferred squared momentum the fixed coupling constant must be replaced by a running coupling constant. This procedure is usually referred as the renormalization-group-improved perturbation, which leads to the absorption of the large logarithmic terms into the running coupling constant. In simple words, given a truncated series of a physical quantity expanded in powers of a coupling constant in a given scheme:

$$R_n = \alpha^s(\mu)[r_0 + r_1(\mu)\alpha(\mu) + \dots + r_n(\mu)\alpha^n(\mu)] \quad , \quad (1)$$

the coupling scale  $\mu$  must be chosen appropriately for the perturbative series to be useful. The unknown dependence of the truncated series on  $\mu$  is commonly referred as the coupling scale ambiguity problem. There is also another source of ambiguity in the perturbative expansion arising from the freedom in the choice of the renormalization scheme. However, in our previous paper we have argued that the scale ambiguity is a more fundamental problem than the corresponding scheme ambiguity, in the sense that if one is able to solve the general scale setting problem, then there is no ambiguity in how to implement different schemes.

Several methods have been proposed to solve the coupling scale ambiguity. Among them we shall mention:

1. *Fastest Apparent Convergence* (FAC):<sup>4,5</sup>

The idea behind FAC is that one should choose the coupling scale that makes the series look like most convergent. Frequently it is defined as the condition of a vanishing second order term (i.e., next to tree level) coefficient. A related topic is the “effective charge”<sup>4</sup> or the “Renormalization Scheme Invariant” (RSI)<sup>6</sup> method, where one effectively requires all higher order coefficients to be zero.

2. *Principle of Minimal Sensitivity* (PMS):<sup>5</sup>

We shall define it here as the choice of the coupling scale at the stationary point of the truncated series:

$$\left. \frac{dR}{d\mu} \right|_{\mu} = 0 \quad . \quad (2)$$

The PMS method also aims toward the choice of a renormalization scheme,

and beyond two-loop order this method requires the variation of scheme parameters besides the coupling scale.

### 3. *Brodsky-Lepage-MacKenzie* (BLM):<sup>7</sup>

This method is inspired from QED. The philosophy is to absorb all fermionic vacuum polarization effects into the running coupling constant. In 1-loop order massless QCD it is operationally equivalent to the condition of a vanishing coefficient of the  $n_f$  (number of light fermions) term. Therefore BLM's results are formally invariant under the change of number of light flavors:

$$\frac{\partial R}{\partial n_f}(\alpha(\mu), n_f) = 0 \quad . \quad (3)$$

The usual impression is that as long as the coupling scale  $\mu^2$  is chosen near the typical scale  $Q^2$  of a given process, the perturbation series would give a reasonable result. We should notice, however, that due to dimensional transmutation (i.e., the presence of  $\Lambda_{QCD}$ ) the correct scale might in some cases not be proportional to  $Q^2$  but rather to some other power of it, or even in a more complicated way. So the naive form of assigning coupling scale to typical physical scales runs the danger of being too simplistic. Also, for processes involving many scales, in general it is not clear how a “typical scale” can be defined.

For multi-scale processes, the conventional way of assigning a uniform coupling throughout all vertices becomes questionable. Consider, for instance, the exclusive process  $e^+e^- \rightarrow \mu^+\mu^-\gamma$  (fig. 1). In QED the vertices **a** and **b** should have a coupling strength  $\sim \alpha^{1/2}(Q^2)$  whereas the vertex involving the radiated photon should have a strength  $\sim \alpha^{1/2}(0) = 1/\sqrt{137}$ .

This observation and the existing controversy on the various scale setting procedures prompt us to explore the Dressed Skeleton Expansion (DSE) instead of the conventional power series expansion. The basic idea of skeleton type calculation is rather simple:

- 1) The basic vertex functions are calculated by using renormalization group equations.<sup>8</sup>
- 2) Any other Green's function is expanded in skeleton graphs of the basic vertices.

One property of this calculational procedure is that it is automatically scale ambiguity free, because there is no exogenous coupling constant. This resembles BLM's observation of the automatic scale setting procedure for QED. Another observation is that the results in DSE calculations are not a simple power series in a coupling constant. In general the results in DSE calculations are expressed directly in terms of functions that involve a scale analogous to  $\Lambda_{QCD}$ . This should not come as a surprise. In fact, the concept of coupling constant is also lost in conventional perturbation theory with scale fixing procedure. In QCD, after scale fixing, the results are directly expressed in term of  $\Lambda_{QCD}$ . In this sense, the coupling constant merely serves as an intermediate device and is discarded after scale fixing. Another argument in favor of the dressed skeleton expansion is that many of the renormalon type contributions<sup>17,18</sup> are automatically resummed into the full propagators and vertex functions, therefore the higher order skeleton results are expected to be less divergent than conventional power series expansion. For a more detail discussion about DSE and the scale setting problem, we refer the reader to our original paper.<sup>1</sup>

## II. Gross-Neveu model in leading $1/N$ expansion

This section is basically motivated by P. M. Stevenson's analysis of the PMS method in the Gross-Neveu model.<sup>9</sup> We shall consider this model with the presence of the auxiliary scalar field  $\sigma$ .<sup>3,10</sup> The Lagrangian density of this model is given by:

$$\mathcal{L} = \bar{\Psi}^a (i\not{\partial}) \Psi_a - \frac{1}{2} \sigma^2 - g_o \bar{\Psi}^a \Psi_a \sigma \quad , \quad a = 1, 2, \dots, N \quad , \quad (4)$$

The bare propagators and vertex functions of this theory are depicted in fig. 2 and are given by:

$$\begin{aligned} -i\Delta_o &= -i \quad , \\ iD_o^a{}_b &= \frac{i\delta^a{}_b}{p^2 + i\varepsilon} \quad , \\ -i\Gamma_o^a{}_b &= -ig_o\delta^a{}_b \quad , \end{aligned} \quad (5)$$

Let us analyse the off-shell fermion four-point function. Although this is not a “physical” quantity in the usual sense (because of its off-shellness), it nevertheless provides a simple Green's function where various ideas about scale fixing methods can be tested. For our purpose, we shall only deal with perturbative quantities and bypass all non-perturbative effects arising from dynamical symmetry breaking.<sup>11</sup> The fermion four-point function to leading order in  $1/N$  has the structure (fig. 3):

$$G(p_1, p_2, p_3, p_4)^{ab}{}_{cd} = -ig_o^2 [\Delta(s)\delta^a{}_c\delta^b{}_d - \Delta(u)\delta^a{}_d\delta^b{}_c] \quad , \quad (6)$$

where  $\Delta(s)$  is the full propagator of the scalar particle to leading order in  $1/N$ .

Notice that for the Gross-Neveu model in the auxiliary scalar field context, every vertex in a given Feynman diagram counts as a negative unit power in  $N$ ,

while every scalar propagator represents a positive unit power in  $N$ . Thus in the leading  $1/N$  expansion there is no vertex nor fermion self-energy corrections, since these effects are higher order in  $1/N$ .<sup>10</sup> Thus only the full scalar propagator multiplied by the squared bare charge needs renormalization. In the following we shall refer to this function as the “charged scalar propagator”. That is, we can choose to “dress up” the charged scalar propagator instead of the three-point vertex function. This resembles the case of QED, where due to the fact that  $Z_1 = Z_2$ ,<sup>7</sup> only the charged photon propagator needs to be renormalized in order to renormalize the bare charge.

Naturally one can insist to “dress up” the three-point function rather than the two-point scalar function. But as we shall see shortly, both procedures will lead to the same result. Let us consider now the first case, more concretely, let us illustrate the application of the renormalization group equation (RGE), temporarily up to sixth order in the bare coupling constant.

The charged scalar propagator to sixth order in  $g_o$  is (fig. 4) :

$$\begin{aligned}
-ig_o^2\Delta(p^2) &\equiv -ig_{\text{DS}}^2(p^2) \\
&= g_o^2 \left\{ -i + (-i) [ig_o^2\Pi(p^2)](-i) + (-i) \left( [ig_o^2\Pi(p^2)](-i) \right)^2 \right\} \quad (7) \\
&= -ig_o^2 \left\{ 1 + g_o^2\Pi(p^2) + g_o^4\Pi^2(p^2) \right\} \quad ,
\end{aligned}$$

where the subscript DS stands for Dressed Skeleton. The vacuum polarization correction is given by (fig. 4)

$$ig_o^2\Pi(p^2) = -(-ig_o)^2(-i)^2 N \int \frac{d^d k}{(2\pi)^d} \frac{\text{Tr}\{\mathbf{k}(\mathbf{k} + \mathbf{p})\}}{k^2(k + p)^2} \quad . \quad (8)$$

A straightforward calculation leads to:

$$\Pi(p^2) = -\frac{N}{\pi} \left( \frac{1}{\hat{\epsilon}} + \log(-p^2 - i\epsilon) \right) , \quad \frac{1}{\hat{\epsilon}} = \frac{1}{\epsilon} - \log 4\pi + \gamma_E , \quad (9)$$

where we have used dimensional regularization in  $d = 2 + 2\epsilon$ . Equation (7) can be rewritten as:

$$g_{\text{DS}}^2(p^2) = g_o^2 + g_o^4 \Pi(p^2) + g_o^6 \Pi^2(p^2) , \quad (10)$$

and by formally inverting this power series

$$g_o^2 = g_{\text{DS}}^2(p^2) - g_{\text{DS}}^4(p^2) \Pi(p^2) + g_{\text{DS}}^6(p^2) \Pi^2(p^2) + O(g_{\text{DS}}^8) . \quad (11)$$

Now let us obtain the RGE for  $g_{\text{DS}}(p^2)$ . The first step is to differentiate equation (10) with respect to the scale variable  $x = \log(-p^2 - i\epsilon)$ . Noting that

$$\frac{d\Pi}{dx} = -\frac{N}{\pi} , \quad (12)$$

we obtain

$$\frac{dg_{\text{DS}}^2}{dx} = g_o^4 \left( -\frac{N}{\pi} \right) + 2g_o^6 \Pi(p^2) \left( -\frac{N}{\pi} \right) , \quad (13)$$

and then the next step is to replace  $g_o$  by  $g_{\text{DS}}$  by means of the equation (11). After this substitution we obtain a finite RGE for  $g_{\text{DS}}^2(p^2)$ :

$$\frac{dg_{\text{DS}}^2}{dx} = -\frac{N}{\pi} \left\{ \left( g_{\text{DS}}^2(p^2) - g_{\text{DS}}^4(p^2) \Pi(p^2) + \dots \right)^2 + 2g_{\text{DS}}^6 \Pi(p^2) \right\} \quad (14)$$

To order  $g_{\text{DS}}^6$ , this equation is simply

$$\frac{dg_{\text{DS}}^2}{dx} = -\frac{N}{\pi} g_{\text{DS}}^4 + O(g_{\text{DS}}^8) , \quad (15)$$

Notice that the order six coefficient has all but vanished. This is a general result for this model: no matter how many terms we start with, all higher order terms

in the RGE (15) will vanish. (This result would be obvious if we had applied the RGE to  $g_{\text{DS}}^{-2}$  instead of  $g_{\text{DS}}^2$ , but here we have chosen to present the RGE for  $g_{\text{DS}}^2$  in order to indicate the procedure for a general field theory.) In other words, we will always obtain the exact infinite order solution:

$$g_{\text{DS}}^2(p^2) = \frac{\pi}{N \log(-p^2/\Lambda_{\text{GN}}^2 - i\varepsilon)} \quad , \quad (16)$$

independent of the number of terms we have included in the original equation for the charged scalar propagator (eq. (7)). This is true even if we have only included the lowest loop correction.

Naturally, we could have chosen to dress up the three-point vertex function rather than the two-point scalar function. But we can see that in this particular model these two approaches are completely equivalent. More specifically, to dress up the vertex function we need to obtain first the effective wavefunction renormalization constant of the scalar propagator:

$$\begin{aligned} -i\Delta(p^2) &= -i + (-i) \left[ i g_o^2 \Pi(p^2) \right] (-i) + \dots \\ &\equiv (-i) Z(p^2) \quad . \end{aligned} \quad (17)$$

Noting that there are no fermion self-energy nor vertex corrections, to renormalize the three-point function we simply multiply the bare vertex function by the square root of the effective scalar wavefunction renormalization constant (fig. 5)

$$-i\tilde{g}_{\text{DS}}(p^2) \equiv -i g_o Z^{1/2}(p^2) \quad , \quad (18)$$

but this implies

$$\tilde{g}_{\text{DS}}^2(p^2) = g_o^2 Z(p^2) = g_{\text{DS}}^2(p^2) \quad . \quad (19)$$

Thus dressing up the three-point vertex amounts exactly to dressing up the charged

scalar two-point function.

The result for the fermion four-point function is obtained by replacing the  $\Delta$  function in the eq. (6) by using:

$$g_o^2 \Delta(s) = g_{\text{DS}}^2(s) = \frac{\pi}{N \log(-s/\Lambda_{\text{GN}}^2 - i\varepsilon)} \quad , \quad (20)$$

Thus, for the massless Gross-Neveu model in leading  $1/N$  expansion, the DSE result is identically equivalent to the exact result. This should be contrasted with conventional perturbative expansion, where the results are not exact even after applying standard scale setting methods. In fig. 6 we plot the symmetrized and the antisymmetrized 4-point function, where the scale has been fixed by applying second and third order PMS scale-scheme setting method. Following the convention given in the ref. 9, these functions are defined by:

$$R_+(s, u) = \frac{g_o^2 N}{2\pi} [\Delta(s) + \Delta(u)] \quad , \quad (21)$$

$$R_-(s, u) = \frac{2g_o^2 N}{\pi \log(u/s)} [\Delta(s) - \Delta(u)] \quad . \quad (22)$$

We do notice that the third-order approximant improves remarkably over the second order approximant, however, these approximants would start to differ from the exact result at higher value of  $u/s$ . Evidently, the conventional scale setting methods fail to give the exact result in this simple model because of the assignment of a single coupling scale to both skeleton graphs. In fact, had the conventional scale setting procedures (FAC, PMS) been applied to the two skeleton graphs individually, they would have given the exact result, too.

What is the moral of the story? The moral of this exercise is that different skeleton diagrams possess individual renormalization properties, and that by separating different skeleton graphs, at least in this case, one obtains a more exact answer.

### III. Massless Thirring Model

The massless Thirring model<sup>12</sup> is simply the Gross-Neveu model with  $N=1$  and without performing the  $1/N$  expansion. This model is well-known to be exactly solvable<sup>12,13</sup>. The main purpose of considering the massless Thirring model here is to illustrate the DSE calculation beyond the tree skeleton level. As before, we shall only be interested in performing perturbative calculations, and all non-perturbative effects (dynamical mass generation, spontaneous symmetry breaking<sup>10,12,13</sup>, etc.) shall be bypassed. Since the vertex correction is no longer trivial, we can not choose to dress up the charged two-point function. Instead, we should perform the RGE on the three-point vertex function. We shall carry out our calculation within the context of dimensional regularization, with  $d = 2 + 2\epsilon$ . To one-loop order, the fermion self-energy correction remains zero (see fig. 7):

$$ig_o^2 \Sigma(p) = (-i)(-ig_o)^2 \int \frac{d^d k}{(2\pi)^d} \frac{i}{\not{k}} = 0 \quad . \quad (23)$$

Hence there is no fermion wavefunction renormalization to this order:

$$Z_f(p) = 1 + O(g_o^4) \quad . \quad (24)$$

The scalar propagator is renormalized exactly like in the case of the Gross-Neveu

model (see fig. 7)

$$\begin{aligned}
-i\Delta(k^2) &= -i + (-i) \left( i g_o^2 \Pi(k^2) \right) (-i) \\
&= -i \left[ 1 - \frac{g_o^2}{\pi} \left( \frac{1}{\hat{\epsilon}} + \log(-p^2 - i\varepsilon) \right) \right] , 
\end{aligned} \tag{25}$$

from here the effective scalar wavefunction renormalization constant is:

$$Z_b(k^2) = 1 - \frac{g_o^2}{\pi} \left( \frac{1}{\hat{\epsilon}} + \log(-p^2 - i\varepsilon) \right) , \quad \frac{1}{\hat{\epsilon}} = \frac{1}{\epsilon} - \log 4\pi + \gamma_E . \tag{26}$$

The vertex correction (fig. 7) is given by:

$$\begin{aligned}
-i g_o^3 \Gamma_1(p, q) &= (-i) (-i g_o^3) \int \frac{d^d r}{(2\pi)^d} \frac{i}{\not{h} + \not{r}} \frac{i}{\not{p} + \not{r}} , \\
\Gamma_1(k^2) &= \frac{1}{4\pi} \left( \frac{1}{\epsilon} - \log 4\pi - 1 + \log(-k^2 - i\varepsilon) \right) .
\end{aligned} \tag{27}$$

Combining the self-energy, vacuum polarization and vertex corrections, we obtain the renormalized vertex function:

$$-i g_{\text{DS}}(k^2) \equiv -i g_o Z_f^{1/2}(q) \left( 1 + g_o^2 \Gamma_1(k^2) \right) Z_f^{1/2}(p) Z_b^{1/2}(k^2) . \tag{28}$$

This equation can be put into the following form:

$$\frac{1}{g_{\text{DS}}^2(k^2)} = \frac{1}{g_o^2} + \frac{1}{2\pi} \left( \frac{1}{\epsilon} - \log 4\pi + 2\gamma_E + 1 + \log(-k^2 - i\varepsilon) \right) . \tag{29}$$

and its solution is given by

$$g_{\text{DS}}^2(k^2) = \frac{2\pi}{\log\left(-k^2/\Lambda_{\text{Th}}^2 - i\varepsilon\right)} . \tag{30}$$

Notice that if we had used the  $1/N$  expansion ( compare with eq. (16) ), we would have erred by an overall factor 2. Also notice that the vertex function to this order

depends exclusively on the squared momentum of the scalar particle. Now, let us use this vertex function to study the two-particle elastic scattering amplitude. Consider the process indicated in fig. 8, where we have chosen the center-of-mass frame to express our kinematics. The corresponding tree skeleton diagrams are indicated in figure 9.

The external fermion wavefunctions are given by:

$$\begin{aligned}
u_1 &= \sqrt{2p} \begin{pmatrix} 1 \\ 0 \end{pmatrix} , & u_2 &= \sqrt{2p} \begin{pmatrix} 0 \\ 1 \end{pmatrix} , \\
\bar{u}_3 &= \sqrt{2p} (0 \ 1) , & \bar{u}_4 &= \sqrt{2p} (1 \ 0) ,
\end{aligned} \tag{31}$$

and the tree level amplitude is simply

$$\begin{aligned}
iM_{tree} &= ig_{\text{DS}}^2(t)(\bar{u}_3 u_1)(\bar{u}_4 u_2) + ig_{\text{DS}}^2(u)(\bar{u}_4 u_1)(\bar{u}_3 u_2) \\
&= i4p^2 g_{\text{DS}}^2(u) \\
&= \frac{i8\pi p^2}{\log(4p^2/\Lambda_{\text{Th}}^2)} .
\end{aligned} \tag{32}$$

The Mandelstam variables have the following values:

$$s = 4p^2, \quad t = 0, \quad u = -4p^2 . \tag{33}$$

The one-loop order skeleton diagram is given in fig. 10. Let us spend sometime to discuss these diagrams. First of all, let us compute the box diagrams in the usual perturbation theory, i.e., using the bare coupling constant at the vertices. By simple power counting argument, one can see that the two diagrams are individually divergent. However, it turns out that the divergences coming from the

two diagrams cancel each other, as one would expect from the renormalizability of the theory. The Feynman integral of these box diagrams is given by:

$$\begin{aligned}
iM_{box} &= g_o^4 \int \frac{d^2k}{(2\pi)^2} \left( \bar{u}_3 \frac{i}{p_1 - \not{k}} u_1 \right) \left( \bar{u}_4 \frac{i}{p_2 + \not{k}} u_2 \right) + \left( \bar{u}_3 \frac{i}{p_1 - \not{k}} u_1 \right) \left( \bar{u}_4 \frac{i}{p_2 - \not{k}} u_2 \right) \\
&= 4p^2 g_o^4 \int \frac{d^2k}{(2\pi)^2} \frac{k^2}{(k - p_1)^2} \left\{ \frac{1}{(k + p_2)^2} - \frac{1}{(k - p_2)^2} \right\} .
\end{aligned} \tag{34}$$

The propagators in these expressions come with the  $+i\varepsilon$  prescription, and in the language of distribution theory they should be interpreted as the sum of a principal value part and a delta function:

$$\frac{1}{k^2 + i\varepsilon} = \text{P.V.} \frac{1}{k^2} - i\pi\delta(k^2) , \tag{35}$$

thus the terms in the integrand in eq. (34) can be classified into the following three types:

- 1) Product of two principal value parts,
- 2) Product of a principal value part with a delta function,
- 3) Product of two delta functions.

By direct calculation, it can be shown that the first two types of terms vanish, thus the net contribution of the box diagrams comes entirely from the double delta function terms. In figure 11 we plot the location of the singularities of the double delta functions. The result after integration has a simple expression:

$$i\mathcal{M}_{box} = p^2 g_o^4 . \tag{36}$$

Now let us return to the dressed skeleton case. We have to replace the bare coupling vertex  $-ig_o$  by the dressed vertex function  $-ig_{DS}(k^2)$ . At high energies ( $p \gg \Lambda_{DS}$ )

the dominant contribution will still be coming from the two double delta points, the reason of this resides in that these two points are located in deep-spacelike and deep-timelike regions, i.e., far away from the light-cone, and in that  $g_{DS}(k^2)$  is a slow varying function at large  $k^2$ . Therefore, the corrections coming from the infrared behavior of the vertex function  $g_{DS}(k^2)$  are expected to be higher-twist in nature.<sup>14</sup> In a sense, we can interpret the two points shown in fig. 11 as the “scale-setting centers” of the skeleton box diagrams. The Landau singularity at  $k^2 = \Lambda_{\text{Th}}^2$  might cause concern about the box integral. But one should bear in mind that this pole actually is located off the real axis due to the presence of the  $+i\epsilon$  term, and as long as we respect this prescription, this pole poses no threat to the finiteness of the box integral. It turns out that box skeleton diagram can be calculated exactly (see Appendix for the calculation and discussion about the box integral):

$$\begin{aligned}
i\mathcal{M}_{\text{box}} &= 4p^2 \int \frac{d^2k}{(2\pi)^2} \frac{k^2}{(k-p_1)^2} \left\{ \frac{1}{(k+p_2)^2} - \frac{1}{(k-p_2)^2} \right\} g_{\text{DS}}^4(k^2) \\
&= 2p^2 \left[ \Psi' \left( 1 - \frac{i}{\pi} \log(2p/\Lambda_{\text{Th}}) \right) - \Psi' \left( \frac{1}{2} - \frac{i}{\pi} \log(2p/\Lambda_{\text{Th}}) \right) \right] ,
\end{aligned} \tag{37}$$

where  $\Psi'$  is the trigamma function.<sup>15</sup> Needless to say, this amplitude is totally free of scale ambiguity: the result of the skeleton box diagrams is directly expressed in terms of  $p$  and  $\Lambda_{\text{Th}}$ , and no exogenous coupling has been invoked in the calculation. In fig. 12 we plot the real and imaginary part of the effective coupling constant  $g_{\text{eff}}(p)$ , and in fig. 13 we plot the Bode diagrams of amplitude and phase for the effective scale  $p_{\text{eff}}(p)$ . These functions are defined by (see eq. (30) and (36)):

$$\begin{aligned}
i\mathcal{M}_{\text{box}}(p) &\equiv p^2 g_{\text{eff}}^4(p) \\
&\equiv p^2 g_{\text{DS}}^4(p_{\text{eff}}) .
\end{aligned} \tag{38}$$

We observe that at high energies the effective scale has, in the language of phasors, an inductive angle of  $45^\circ$ . This is expected since one box diagram probes into the deep timelike region while the other box diagrams probes into the deep spacelike region (see fig. 11). Thus the effective scale is expected to be half inductive and half resistive. In contrast with conventional scale setting methods, the effective scales and the effective coupling constants in DSE are in general complex numbers.

The total amplitude to one-loop skeleton level is given by the simple addition of the tree-level amplitude (eq. (32) ) and the box amplitude (eq. (37) ):

$$i\mathcal{M}_{tot} = i\mathcal{M}_{tree} + i\mathcal{M}_{box} . \quad (39)$$

#### IV. Yukawa Interaction in 1+1 Dimension

The main purpose in using the Yukawa model here is to present the subtleties related to the mass renormalization of propagators and to the matrix structure of vertex functions. While the usage of the skeleton technique for massless scalar bosons is straightforward, the presence of mass term and the existence of matrix structure in the various basic vertex functions make the extension of the DSE not immediately trivial. The Yukawa model is chosen because it presents these two features at first-loop level. Although the Yukawa model in  $1 + 1$  dimension is a superrenormalizable theory, this does not affect our discussion of Dirac structure. The Yukawa theory describes the interaction between a fermion field and a scalar

boson field according to the following Lagrangian density:

$$\mathcal{L} = \bar{\Psi}(i\not{\partial} - m_f)\Psi + \frac{1}{2}(\partial^2 - m_b^2)\phi^2 + \lambda_o m \bar{\Psi}\Psi\phi . \quad (40)$$

where a mass unit  $m$  has been inserted in the interaction term to make the bare coupling  $\lambda_o$  dimensionless. To simplify our discussion, we shall consider the case of equal renormalized fermion and boson mass, and we further chose  $m$  to have this value. That is, we will take the physical mass of the boson and the fermion to be equal to  $m$ . The bare interaction vertex is scalar (diagonal), in the sense that it is given by  $-\lambda_o m$  and thus proportional to the identity matrix. However, this feature is spoiled by the presence of higher order corrections. The full vertex function will in general contain non-trivial Dirac structure (fig. 14):

$$-im\Lambda(p, q) = -im \left\{ \tilde{\Lambda}_o + \tilde{\Lambda}_1(p, q)\not{p} + \tilde{\Lambda}_2(p, q)\not{q} + \tilde{\Lambda}_3(p, q)\not{p}\not{q} \right\} . \quad (41)$$

In general the vertex function  $\Lambda(p, q)$  will be an  $N$  by  $N$  matrix, and an immediate question is how to apply DSE method to obtain all the  $N^2$  components of this vertex function. A first approach would be to write down the RGEs for all the components and solve them separately. But this would introduce  $N^2$  integration constants, that is,  $N^2$  quantities analogous to  $\Lambda_{\text{QCD}}$ . This is hardly necessary, for we know that, aside from the masses of the particles, we only need one more parameter to fix the entire theory. Therefore we can solve the RGE for only one component, and then expand the other components in term of the one we have solved for.

The next question is how to choose the component for the RGE. One obvious

selection is  $\tilde{\Lambda}_o$ , for we know that in weak coupling regime the vertex function should somehow resemble the bare coupling, which is scalar diagonal. More precisely, we

1) solve the RGE for  $\tilde{\Lambda}_o(p, q)$

$$\tilde{\Lambda}_o(p, q) = \lambda_o (1 + f_1(p, q)\lambda_o^2 + f_2(p, q)\lambda_o^4 + \dots) \quad , \quad (42)$$

2) expand the other components in power series of  $\tilde{\Lambda}_o(p, q)$  by inverting the equation (42). For example,  $\tilde{\Lambda}_1$  will have the expression

$$\begin{aligned} \tilde{\Lambda}_1(p, q) &= h_1(p, q)\lambda_o^3 + h_2(p, q)\lambda_o^5 + \dots \\ &= h_1(p, q)\Lambda_o^3(p, q) + (h_2(p, q) - 3f_1(p, q))\Lambda_o^5(p, q) + \dots \end{aligned} \quad (43)$$

While this procedure is formally valid, we notice that the four matrices  $\{\mathbf{1}, \not{p}, \not{q}, \not{p}\not{q}\}$  are not the most desirable choice of basis to decompose  $\Lambda$ . The problem is that when  $p$  and  $q$  are on-shell and the vertex function is multiplied by the external fermion wavefunctions, the matrices  $\not{p}$  and  $\not{q}$  can be formally replaced by the scalar matrix  $m \cdot \mathbf{1}$  because the wavefunctions satisfy Dirac equation. This means that, on-shell, the matrices  $\not{p}$  and  $\not{q}$  are indistinguishable from a scalar matrix. Thus, it is highly unnatural to perform the RGE on  $\tilde{\Lambda}_o$ , for it means that its on-shell value will not be representative of the entire vertex function. Therefore, we are lead to the more natural choice of basis matrices given by:  $\{\mathbf{1}, \not{p} - m, \not{q} - m, (\not{q} - m)(\not{p} - m)\}$ .<sup>16</sup> Notice that now the non-scalar components vanish on-shell upon contraction with the external fermion wavefunctions because of Dirac equation, thus the on-shell value of the vertex function is completely contained in the scalar component.

Let us carry out the explicit computation of these components of the vertex function in DSE to 1-loop order. The scalar boson propagator offers no major difficulty: we simply absorb all renormalization effect into the effective wavefunction renormalization constant  $Z_b$  (fig. 14)

$$i\Delta_b(p^2) = \frac{i}{p^2 - m_b^2} + \frac{i}{p^2 - m_b^2} i\lambda_o^2 m^2 \Pi(p^2) \frac{i}{p^2 - m_b^2} + \dots \quad , \quad (44)$$

$$i\lambda_o^2 m^2 \Pi(r^2) = (-1)(-i\lambda_o m)^2 (i)^2 \int \frac{d^d k}{(2\pi)^d} \frac{\text{Tr} [(\not{k} + \not{r} + m_f)(\not{k} + m_f)]}{[(k+r)^2 - m_f^2][k^2 - m_f^2]} \quad . \quad (45)$$

To the lowest order, we can replace the bare fermion mass  $m_f$  by  $m$  in the previous expression, and obtain

$$\Pi(r^2) = \frac{1}{4\pi} \left( \frac{1}{\hat{\epsilon}} + \int_0^1 dx \log(-x(1-x)r^2 + m^2 - i\varepsilon) \right) \quad . \quad (46)$$

The bare boson mass to order  $\lambda_o^2$  is given by

$$m_b^2 = m^2(1 + \lambda_o^2 c_b) \quad , \quad (47)$$

where  $c_b$  is the lowest order counterterm. Replacing (46) and (47) into (44), and retaining only terms to order  $\lambda_o^2$ , we obtain the expression

$$i\Delta_b(r^2) = \frac{i}{r^2 - m^2} \left( 1 + \lambda_o^2 m^2 \frac{c_b - \Pi(r^2)}{r^2 - m^2} \right) \quad . \quad (48)$$

On mass shell ( $r^2 = m^2$ ),  $\Delta_b$  has a simple pole, therefore  $c_b = \Pi(m^2)$ , and

$$i\Delta_b(r^2) = \frac{i}{r^2 - m^2} \left( 1 - \lambda_o^2 m^2 \frac{\Pi(r^2) - \Pi(m^2)}{r^2 - m^2} \right) \equiv \frac{i}{r^2 - m^2} Z_b(r^2) \quad . \quad (49)$$

The effective wavefunction renormalization constant is given by

$$Z_b(r^2) = 1 - \lambda_o^2 m^2 \frac{\Pi(r^2) - \Pi(m^2)}{r^2 - m^2} . \quad (50)$$

In particular, the on-shell renormalization constants is

$$Z_{b-OS} = Z_b(m^2) = 1 - \lambda_o^2 m^2 \left. \frac{d\Pi}{dr^2} \right|_{r^2=m^2} = 1 + \frac{\lambda_o^2}{4\pi} \left( \frac{2\pi}{3\sqrt{3}} - 1 \right) . \quad (51)$$

For the fermion propagator we apply a similar procedure (fig. 14). To one-loop order

$$i\mathbf{D}_f(q) = \frac{i}{\not{q} - m_f} + \frac{i}{\not{q} - m_f} \left( i\lambda_o^2 m^2 \Sigma(q) \right) \frac{i}{\not{q} - m_f} . \quad (52)$$

where the self-energy is given by

$$i\lambda_o^2 m^2 \Sigma(q) = (-i\lambda_o m)^2 (i)^2 \int \frac{d^d k}{(2\pi)^d} \frac{\not{k} + m}{[(k-p)^2 - m_b^2][k^2 - m_f^2]} . \quad (53)$$

To order  $\lambda_o^2$  (for  $\mathbf{D}_f(q)$ ), we can replace the boson mass  $m_b$  by  $m$ . After removing the mass counterterm for the fermion mass

$$m_f^2 = m^2(1 + \lambda_o^2 c_f) , \quad (54)$$

by requiring  $\mathbf{D}_f(q)$  to have a simple pole at  $q^2 = m^2$ , we obtain the following

expression for the full fermion propagator

$$\begin{aligned}
i\mathbf{D}_f(q) &= \mathbf{Z}_f(q) \frac{i}{\not{q} - m} \quad , \\
\mathbf{Z}_f^{1/2}(q) &= 1 - \frac{\lambda_o^2 (q^2 + m^2) f(q^2) - 2m^2 f(m^2)}{8\pi (q^2 - m^2)} \\
&\quad - \frac{\lambda_o^2 f(q^2) - f(m^2)}{8\pi (q^2 - m^2)} m(\not{q} - m) \quad , \\
f(q^2) &= \frac{m^2}{\sqrt{q^2(q^2 - 4m^2 + i\varepsilon)}} \left[ \log \left( 1 - \sqrt{\frac{p^2}{p^2 - 4m^2 + i\varepsilon}} \right) \right. \\
&\quad \left. - \log \left( 1 + \sqrt{\frac{p^2}{p^2 - 4m^2 + i\varepsilon}} \right) \right] \quad .
\end{aligned} \tag{55}$$

Notice that instead of a scalar (diagonal) wavefunction renormalization constant, we have introduced an effective wavefunction renormalization matrix. The on-shell expression of this matrix is

$$\begin{aligned}
\mathbf{Z}_{f-OS}^{1/2}(p) &= \mathbf{Z}_f^{1/2}(p)|_{p^2=m^2} \\
&= 1 - \frac{\lambda_o^2}{8\pi} \left( \frac{2}{3} + \frac{\pi}{9\sqrt{3}} \right) - \frac{\lambda_o^2}{8\pi} \left( \frac{1}{3} - \frac{\pi}{9\sqrt{3}} \right) \frac{\not{p} - m}{m} \quad ,
\end{aligned} \tag{56}$$

where the scalar part ( the first two terms ) is readily identified as the conventional on-shell wavefunction renormalization constant. The last term vanishes on-shell upon contraction with the associated external fermion wavefunction.

Let us study the full vertex function at the particular configuration  $p^2 = r^2 = m^2$  and spacelike  $q^2 = -Q^2 < 0$ . The vertex function at a general momentum configuration could be studied exactly the same manner, but the expressions involved would be much more complicated.

The vertex correction (fig. 14) is given by

$$-i\lambda_o^3 m \Gamma_1 = (-i\lambda_o m)^3 \int \frac{d^d k}{(2\pi)^d} \frac{(i)^3 (\not{k} + \not{h} + m)(\not{k} + \not{p} + m)}{[(k+q)^2 - m^2][(k+p)^2 - m^2][k^2 - m^2]}, \quad (57)$$

where we have set  $m_f = m_b = m$ . The decomposition of  $\Gamma_1$  into the various components is given by

$$\Gamma_1(q^2) = \frac{1}{4\pi} \left\{ h_o(q^2) \mathbf{1} + h_1(q^2) \frac{\not{p} - m}{m} + h_2(q^2) \frac{\not{h} - m}{Q} + h_3(q^2) \frac{(\not{h} - m)(\not{p} - m)}{Q \cdot m} \right\} \quad (58)$$

with

$$\begin{aligned} h_o(q^2) &= 3 \int_0^1 dx \int_0^x dy \frac{x-y}{D^2}, \\ h_1(q^2) &= \int_0^1 dx \int_0^x dy \frac{1+x-3y}{D^2}, \\ h_2(q^2) &= \frac{Q}{m} \int_0^1 dx \int_0^x dy \frac{-1+3x-y}{D^2}, \\ h_3(q^2) &= \frac{Q}{m} \int_0^1 dx \int_0^x dy \frac{x-y}{D^2}, \\ D &= 1 - y + y^2 - (1-x)(x-y) \frac{q^2}{m^2} - i\varepsilon. \end{aligned} \quad (59)$$

The renormalized vertex function is given by

$$-im\Lambda(p, q) = -i\lambda_o m \mathbf{Z}_f^{1/2}(q) (1 + \lambda_o^2 \Gamma_1) \mathbf{Z}_{f-OS}^{1/2}(p) \mathbf{Z}_{b-OS}^{1/2}. \quad (60)$$

Upon decomposition we have

$$\begin{aligned} \Lambda(p, q) &= \lambda_{DS}(q^2) \cdot \mathbf{1} + \lambda_1(q^2) \frac{\not{p} - m}{m} + \lambda_2(q^2) \frac{\not{h} - m}{Q} \\ &\quad + \lambda_3(q^2) \frac{(\not{h} - m)(\not{p} - m)}{Q \cdot m}. \end{aligned} \quad (61)$$

where we have named the scalar component the dressed skeleton effective coupling constant. It satisfies the RGE

$$\frac{1}{\lambda_{\text{DS}}^2(q^2)} = \frac{1}{\lambda_o^2} + \frac{1}{4\pi} \left[ \frac{(q^2 + m^2)f(q^2) - 2m^2f(m^2)}{2(q^2 - m^2)} + \frac{5}{3} - \frac{5\pi}{9\sqrt{3}} + 2h_o(q^2) \right] , \quad (62)$$

with the solution

$$\lambda_{\text{DS}}^2(q^2) = \frac{\lambda^2}{1 + (\lambda^2/4\pi)L(q^2)} , \quad (63)$$

$$L(q^2) = \frac{q^2 + m^2}{2(q^2 - m^2)} f(q^2) - \frac{\pi}{3\sqrt{3}} \frac{m^2}{q^2 - m^2} + 2h_o(q^2) + \frac{3}{4} - \frac{5\pi}{3\sqrt{3}} .$$

we have chosen the integration constant  $\lambda$  such that  $L(q^2 = 0^-) = 0$ . That is,  $\lambda$  is the effective coupling at zero spacelike momentum

$$\lambda_{\text{DS}}(q^2 = 0^-) = \lambda . \quad (64)$$

The general procedure to obtain the other three components involves an expansion of  $\lambda_o$  in term of  $\lambda_{\text{DS}}(q^2)$  by inverting the eq. (62), and then using this substitution in the eq. (61). But to this order we simply need to replace  $\lambda_o$  in the eq. (61) by  $\lambda_{\text{DS}}$ . The resulting expressions are:

$$\begin{aligned} \lambda_1(q^2) &= \frac{\lambda_{\text{DS}}^3(q^2)}{4\pi} \left( h_1(q^2) - \frac{1}{6} + \frac{\pi}{18\sqrt{3}} \right) , \\ \lambda_2(q^2) &= \frac{\lambda_{\text{DS}}^3(q^2)}{4\pi} \left( h_2(q^2) - \frac{1}{2} mQ \frac{f(q^2) - f(m^2)}{q^2 - m^2} \right) , \\ \lambda_3(q^2) &= \frac{\lambda_{\text{DS}}^3(q^2)}{4\pi} h_3(q^2) . \end{aligned} \quad (65)$$

In figure 15 we plot the different components of the full vertex function for two different values of  $\lambda$ . Notice that in the weak coupling regime (say,  $\lambda^2/4\pi < 0.2$ ),

the renormalization effects become small, namely, the scalar component at high energy only gets slightly renormalized, and the non-scalar ones become comparatively negligible.

## V. Summary

We have analysed the application of the DSE to simple field theory models in  $1 + 1$  dimension and discussed the various technical features in its implementation. Among the main conclusions we should mention:

- 1) In the Gross-Neveu model, the DSE is equivalent to the exact result. We argue that the failure of conventional scale setting methods (FAC, PMS) to yield the exact result resides in the assignment of a uniform coupling scale to different skeleton graphs.
- 2) We have shown in the Thirring model that loop skeleton diagrams can be meaningfully computed. For asymptotic free theories like QCD, we indicate that the presence of the Landau singularity at  $\Lambda_{QCD}$  is not expected to pose threat to loop skeleton integrals, as long as the  $+i\epsilon$  prescription is carefully respected. Also, the effective scale of loop skeleton diagrams is shown to be coming from deep timelike and spacelike regions, thus the detail infrared behavior of the vertex function gives only higher twist correction.
- 3) We have extended the DSE to vertex functions involving Dirac matrix structure. For the fermion-boson interaction vertex, we have pointed out that one should perform the RGE on the scalar component ( $\lambda_{DS}$ ) of the vertex function, with the exclusion of those components that vanish on-shell upon

contraction with external fermion wavefunctions. Once the scalar component is obtained, the non-scalar ones are to be expanded in power series of the scalar component.

Application of DSE to scale setting for the three-gluon vertex in QCD is discussed in a forthcoming paper.

We thank Prof. Stanley Brodsky for the suggestion of the scale setting problem and helpful discussions. We also thank helpful discussions with Matthias Burkardt, Carl J. Im, Carlos A. R. Sá de Melo, Jorge G. Russo and Brian J. Warr.

### Appendix: Box Diagram Calculation

The skeleton box diagrams indicated in fig. 9 gives the following Feynman integral:

$$i\mathcal{M}_{box} = 4p^2 \int \frac{d^2k}{(2\pi)^2} \frac{k^2}{(k-p_1)^2} \left\{ \frac{1}{(k+p_2)^2} - \frac{1}{(k-p_2)^2} \right\} \frac{4\pi^2}{\log^2(-k^2/\Lambda_{Th}^2 - i\varepsilon)} \quad (66)$$

To perform this integral, let us first expand the inverse square of the logarithm into power series in  $\log(p^2/\Lambda_{Th}^2)$ . Define

$$x = \log(p^2/\Lambda_{Th}^2) , \quad \hat{k} = k/p , \quad (67)$$

we have

$$\begin{aligned} \log^{-2} \left( -\frac{k^2}{\Lambda_{Th}^2} - i\varepsilon \right) &= \left[ \log \left( \frac{p^2}{\Lambda_{Th}^2} \right) + \log \left( -\frac{k^2}{p^2} - i\varepsilon \right) \right]^{-2} \\ &= \left[ x + \log(-\hat{k}^2 - i\varepsilon) \right]^{-2} \\ &= \frac{1}{x^2} \sum_{n=0}^{\infty} \binom{-2}{n} \frac{\log^n(-\hat{k}^2 - i\varepsilon)}{x^n} , \end{aligned} \quad (68)$$

where

$$\binom{-2}{n} = \frac{(-2)(-3)\dots(-1-n)}{1 \cdot 2 \cdot \dots \cdot n} = (-1)^n (n+1) \quad . \quad (69)$$

This expansion effectively corresponds to the expansion of the box skeleton diagrams into a power series in the coupling constant at scale  $p$ .

By applying the identity:

$$\log^n(-\hat{k}^2 - i\varepsilon) = \left( \frac{\partial}{\partial \alpha} \right)_{\alpha=0}^n (-\hat{k}^2 - i\varepsilon)^\alpha \quad , \quad (70)$$

the Feynman integrals can be done exactly, the result is:

$$\begin{aligned} i\mathcal{M}_{box} &= \frac{4\pi^2 p^2}{x^2} \sum_{n=0}^{\infty} (-1)^n \frac{n+1}{x^n} \left( \frac{\partial f}{\partial \alpha} \right)_{\alpha=0}^n \\ &= \frac{4\pi^2 p^2}{x^2} \{1 - 2!f_1 x^{-1} + \dots + (-1)^n (n+1)!f_n x^{-n} + \dots\} \quad , \end{aligned} \quad (71)$$

where

$$f(\alpha) = (4i)^\alpha \sec\left(\frac{\pi\alpha}{2}\right) = f_0 + f_1\alpha + f_2\alpha^2 + \dots \quad , \quad (72)$$

We give here the numerical value of the first few coefficients:

$$\begin{aligned} f_0 &= 1 \\ f_1 &= 1.38629 + i1.5708 \\ f_2 &= 0.960906 + i2.17759 \\ f_3 &= 0.444033 + i2.80132 \\ f_4 &= 0.15389 + i2.48848 \\ f_5 &= 0.0426674 + i2.75823 \\ f_6 &= 0.00985826 + i2.40832 \quad . \end{aligned} \quad (73)$$

The expansion (71) exhibits an  $n!$  divergence behavior, typical of an asymptotic

series that needs Borel resummation<sup>17,19</sup> in order to yield a finite result.<sup>20</sup> It turns out that this series can be Borel resummed exactly, and the result obtained by a straightforward application of the Borel resummation formulas is given by:

$$i\mathcal{M}_{box} = 2p^2 \left[ \Psi' \left( 1 - \frac{i}{\pi} \log(2p/\Lambda_{\text{Th}}) \right) - \Psi' \left( \frac{1}{2} - \frac{i}{\pi} \log(2p/\Lambda_{\text{Th}}) \right) \right] , \quad (74)$$

where  $\Psi'$  is the trigamma function<sup>15</sup> defined by

$$\begin{aligned} \Psi'(z) &= \frac{d\Psi}{dz} = \frac{d^2}{dz^2} \log \Gamma(z) \\ &\sim \frac{1}{z} + \frac{1}{2z^2} + \frac{1}{6z^3} - \frac{1}{30z^5} + \frac{1}{42z^7} - \frac{1}{30z^9} + \dots \end{aligned} \quad (75)$$

It is interesting to observe that the Borel transform of the series (71):

$$G(y) \sim \delta(y) + \frac{d^2}{dy^2} (yf(-y)) , \quad (76)$$

possesses infinite number of poles on the real axis (see fig. 16). These poles exhibit the typical feature of renormalon singularities<sup>17,21</sup>. We notice that these poles lie exactly on the real axis, i.e., they do not have infinitesimal imaginary part. Thus, when performing the Borel integral, those poles on the positive real axis should be interpreted in the principal value sense. We note that the resulting integral under this prescription is finite.

## REFERENCES

1. H. J. Lu and C. A. R. Sá de Melo, SLAC-PUB-5534.
2. M. Korowski, in “*The Ways of Subnuclear Physics*”, ed. A. Zichichi, (Plenum Press, New York, 1979),  
A. B. Zamolodchikov and A. B. Zamolodchikov,  
*Nuc. Phys.* **B133**, 525 (1978); *Phys. Lett.* **72B**, 481 (1978); *Ann. Phys.* **120**, 253 (1979),  
R. Shankar and E. Witten, *Nuc. Phys.* **B141**, 349 (1978),  
B. Berg and P. Weisz, *Nuc. Phys.* **B146**, 205 (1978),  
M. Karowski, *Nuc. Phys.* **B153**, 244 (1979),  
E. Abdalla, B. Berg and P. Weisz, *Nuc. Phys.* **B157**, 387 (1979),  
M. Karowski, H. J. Thun, *Nuc. Phys.* **B190**, 61 (1981).
3. D. J. Gross and A. Neveu, *Phys. Rev.* **D10**, 3235 (1974).
4. G. Grunberg *Phys. Lett.* **95B**, 70 (1980); *Phys. Lett.* **110B**, 501(E) (1982);  
*Phys. Rev.* **D29**, 2315 (1984).
5. P. M. Stevenson, *Phys. Lett.* **100B**, 61 (1981); *Phys. Rev.* **D23**, 2916 (1981);  
*Nuc. Phys.* **B203**, 472 (1982); *Nuc. Phys.* **B231**, 65 (1984).
6. A. Dhar, *Phys. Lett.* **128B**, 407 (1983),  
A. Dhar and V. Gupta, *Pramana* **21**, 207 (1983),  
A. Dhar and V. Gupta, *Phys. Rev.* **D29**, 2822 (1984),  
V. Gupta, D. V. Shirkov and O. V. Tarasov, TIFR/TH/90-19.
7. S. J. Brodsky, G. P. Lepage and P. B. Mackenzie, *Phys. Rev.* **D28**, 228 (1983).

8. The actual implementation of the DSE depends on the specific field theory model. In general the renormalization effects of two-point functions can be absorbed into effective wavefunction renormalization constants, and the renormalization group equation is applied directly on the vertex function. However, in some instances, e.g. in QED (where  $Z_1 = Z_2$ ) or in the massless Gross-Neveu model in leading  $1/N$  expansion, one can alternatively choose to dress up the “charged two-point function” instead of the vertex function.
9. Application of the PMS scale-scheme setting procedure to the Gross-Neveu model has been studied by P. M. Stevenson, *Phys. Rev.* **D24**, 1622 (1981).
10. An elementary introduction to the  $1/N$  expansion can be found in S. Coleman, “*Aspects of Symmetry*”, Cambridge University Press, 1985.
11. See ref. 3, 10 and  
 S. Coleman and E. Weinberg, *Phys. Rev.* **D7**, 1888 (1973),  
 S. Coleman, *Phys. Rev.* **D10**, 2491 (1974).
12. W. E. Thirring, *Ann. Phys.* **3**, 91 (1958); *Nuovo. Cim.* **9**, 1007 (1958).
13. V. Glaser, *Nuovo. Cim.* **9**, 990 (1958),  
 K. Johnson, *Nuovo. Cim.* **20**, 773 (1961),  
 H. Leutwyler, *Helv. Phys. Acta* **38**, 431 (1965),  
 F. A. Berezin, “*The method of Second Quantization*”, Academic Press, New York, 1966,  
 A. V. Astakhov, O. I. Zav’yalov and A. D. Sukhanov, *JETP* **25**, 512 (1967),  
 G. F. Dell’Antonio, Y. Frishman and D. Zwanziger, *Phys. Rev.* **D6**, 988 (1972),

A. K. Pogrebkov, *Theor. Math. Phys.* **17**, 977 (1973),

P. de Mottoni, *Ann. Inst. Henri Poincaré, Sect. A*, **16**, 265 (1972).

The equivalence between quantum sine-Gordon model with the massive Thirring model is discussed in:

S. Coleman, *Phys. Rev.* **D11**, 2088 (1975),

S. Mandelstam, *Phys. Rev.* **D11**, 3026 (1975),

A. Luther, *Phys. Rev.* **B14**, 2153 (1976).

14. In ref. 9 it is pointed out that in the Gross-Neveu case the Landau pole at  $k^2 = \Lambda_{\text{GN}}^2$  is unphysical and that when the spontaneous symmetry breaking effects are taken into account, the logarithm that appears in the vertex function should be replaced by

$$B(s, M^2) = \left( \frac{s + 4M^2}{s} \right)^{1/2} \log \left( \frac{(s + 4M^2)^{1/2} + \sqrt{s}}{(s + 4M^2)^{1/2} - \sqrt{s}} \right), \quad (77)$$

where  $M$  is the dynamically generated fermion mass. This substitution will yield correction of the order  $M^2/s$ , which becomes negligible in the large  $s$  limit.

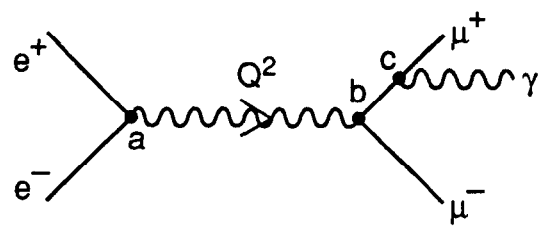
15. M. Abramowitz and I. A. Stegun, “*Handbook of Mathematical Functions*”, (Dover Publications Inc., New York, 1972).
16. This is by no means the unique choice. In fact, any  $m$  in this expression can be replaced by a smooth function of  $p$  and  $q$ , as long as the on-shell value of this function is  $m$ . However, we have preferred “static” basis matrices on the ground of simplicity.
17. G. 't Hooft, in “*The Ways of Subnuclear Physics*”, ed. A. Zichichi, (Plenum Press, New York, 1979).

18. B. Lautrup, *Phys. Lett.* **69B**, 109 (1977),  
P. Olesen, *Phys. Lett.* **73B**, 327 (1978).
19. Application of Borel resummation technique to  $\phi^4$ -field theory in various dimensions can be found in:  
L. N. Lipatov, *Pis'ma Zh. Eksp. Theor. Fiz.* **25**, 116 (1977) (*JETP Lett.* **25**, 104),  
G. 't Hooft, *Phys. Lett.* **119B**, 369 (1982),  
J. Zinn-Justin, *Phys. Rept.* **70**, 109 (1981) .
20. However, in the large  $x$  limit, this asymptotic series still provides a good approximation to the exact result, as long as we stop summing the series at the term where the series begins to diverge. More precisely, for large  $x$ , the first few terms of the series will present an apparent convergence, until the term where  $x^n \sim n!$ . See ref. 17 for further discussion on this point and for an elementary introduction to Borel resummation.
21. G. Parisi, *Nuc. Phys.* **B150**, 163 (1979),  
A. H. Mueller, *Nuc. Phys.* **B250**, 327 (1985).

## FIGURE CAPTIONS

- 1) A typical QED process, where the coupling strength at vertices **a** and **b** is expected to be stronger than the coupling strength at **c**.
- 2) Bare propagators and coupling vertex of the massless Gross-Neveu model.
- 3) The fermion four-point function to leading order in  $1/N$ . The double dashed line represents the full scalar propagator to leading order in  $1/N$ .
- 4) The charged scalar propagator and the vacuum polarization diagrams in Gross-Neveu model to leading order in  $1/N$ .
- 5) Dressed three-point function in Gross-Neveu model to leading order in  $1/N$ .
- 6) Symmetrized ( $R_+$ ) and antisymmetrized ( $R_-$ ) fermion four-point functions to leading order in  $1/N$  in Gross-Neveu model. The dashed lines represent the exact results. The solid lines are the results obtained by applying the PMS optimization method. Fig. (a) and fig. (b) correspond respectively to the second and the third order approximant.
- 7) One-loop self-energy, vacuum polarization and vertex correction diagrams in massless Thirring model.
- 8) Kinematics of two-particle elastic collision process in massless Thirring model in the center-of-mass frame.
- 9) Tree-skeleton diagrams for two-particle elastic scattering amplitude in massless Thirring model.
- 10) One-loop skeleton diagram for two-particle elastic scattering amplitude in massless Thirring model.

- 11) Location of the double-delta function singularities of the box diagrams (a) and (b) of fig. 10 in the  $k_0 - k_1$  plane. The hyperbola indicates the location of the Landau singularity at  $k^2 = -\Lambda_{\text{TH}}^2$ .
- 12) Real and imaginary parts of the effective coupling constant for the box amplitude of the Thirring model. Notice that at high energy  $g_{eff}(p) \rightarrow g_{\text{DS}}(p)$ .
- 13) (a) Bode diagram of amplitude for the effective scale of the box amplitude in the Thirring model. (b) Bode diagram of phase for the effective scale of the same amplitude.
- 14) One-loop scalar and fermion propagator and vertex correction diagrams for the Yukawa model.
- 15) Different components of the full vertex function of Yukawa model in  $1 + 1$  dimension as obtained by DSE. The external legs of the scalar boson and one of the fermions are on-shell; the second fermion has a spacelike momentum  $q^2 = -Q^2 < 0$ . In fig. (a)  $\lambda^2/4\pi = 1/\pi = 0.318$ . In fig. (b)  $\lambda^2/4\pi = 0.2$ .
- 16) Location of the singularities of the Borel transform of the box amplitude in the complex- $y$  plane. There is a delta function at the origin and an infinite number of poles located at odd integer numbers, which correspond to renormalon singularities.



6-91

6952A1

Fig 1

$$\bullet \text{---} \bullet = -i\Delta_0 = -i$$

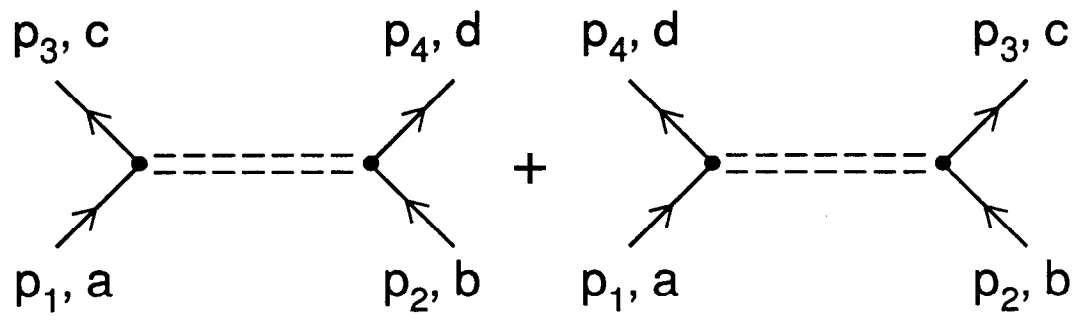
$$\begin{array}{c} \text{b} \qquad \qquad \text{a} \\ \bullet \text{---} \bullet \\ \qquad \qquad \qquad \text{p} \end{array} = iD_{0b}^a = \frac{i\delta_b^a}{p^2 + i\epsilon}$$

$$\begin{array}{c} \text{a} \\ \nearrow \\ \bullet \\ \nwarrow \\ \text{b} \end{array} \text{---} \text{wavy} = -i\Gamma_{0b}^a = -ig_0\delta_b^a$$

6-91

6952A2

Fig 2



6-91

6952A3

Fig 3

$$\begin{aligned}
 -i g_{DS}(p^2) &= g_0^2 \bullet \text{-----} \bullet \\
 &= g_0^2 \left[ \bullet \text{-----} \bullet + \bullet \text{-----} \circ \text{-----} \bullet \right. \\
 &\quad \left. + \bullet \text{-----} \circ \text{-----} \circ \text{-----} \bullet + \dots \right] \\
 \text{---} \xrightarrow{p} \bullet \begin{array}{c} \text{---} \xrightarrow{k} \circ \xrightarrow{k+p} \text{---} \\ \text{---} \xrightarrow{k+p} \bullet \end{array} &= i g_0^2 \Pi(p^2)
 \end{aligned}$$

6-91  
6952A4

Fig 4

$$-i\tilde{g}^{DS}(p^2) = \left[ \begin{array}{c} \diagup \\ \bullet \\ \diagdown \end{array} \rightarrow \text{---} p^2 \text{---} \right] Z^{1/2}(p^2)$$

6-91

6952A5

Fig 5

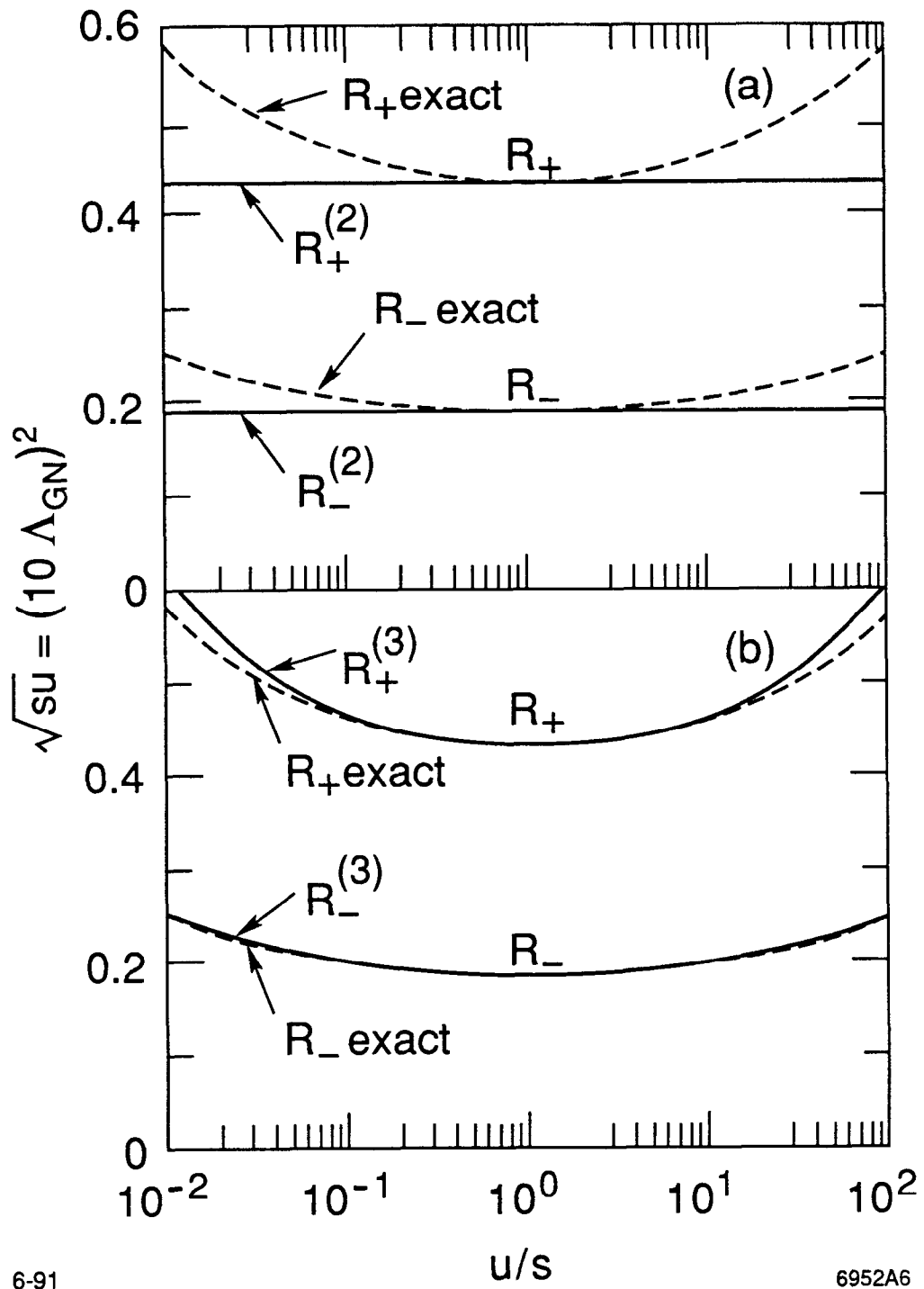
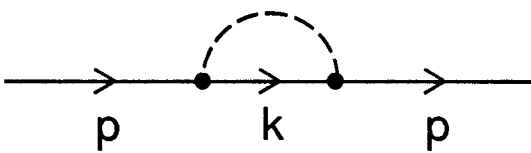
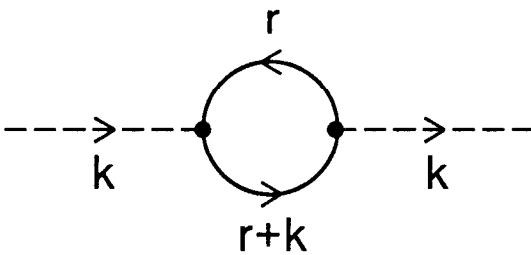
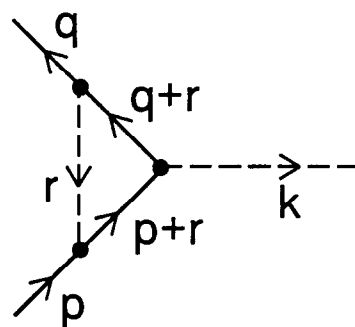


Fig 6

$$ig_0^2 \Sigma(p) =$$


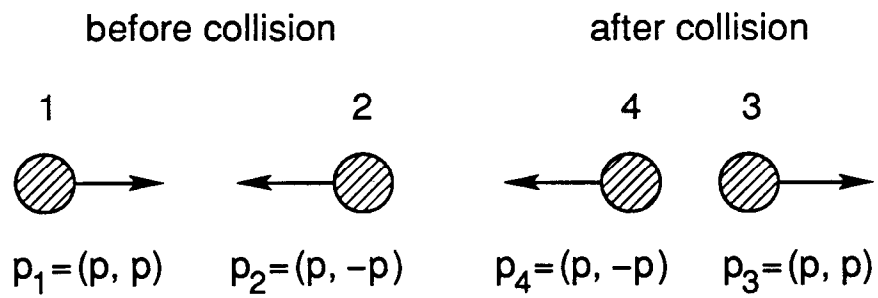
$$ig_0^2 \Pi(k^2) =$$


$$-ig_0^3 \Gamma_1(k^2) =$$


6-91

6952A7

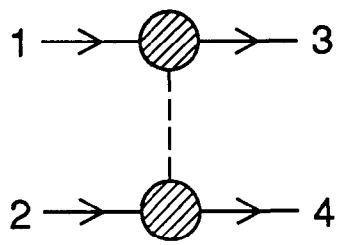
Fig 7



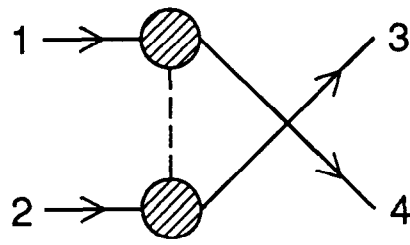
6-91

6952A8

Fig 8

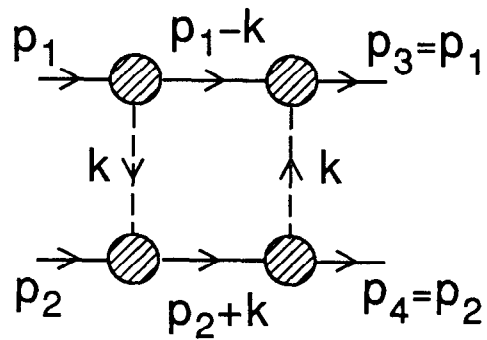


6-91



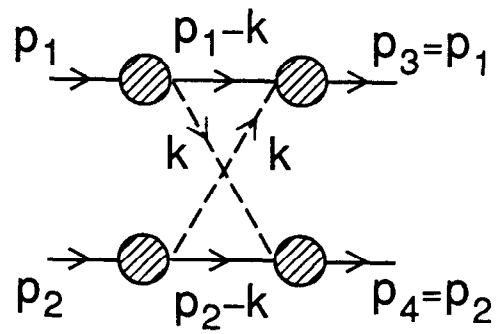
6952A9

Fig 9



6-91

(a)



6952A10

(b)

Fig 10

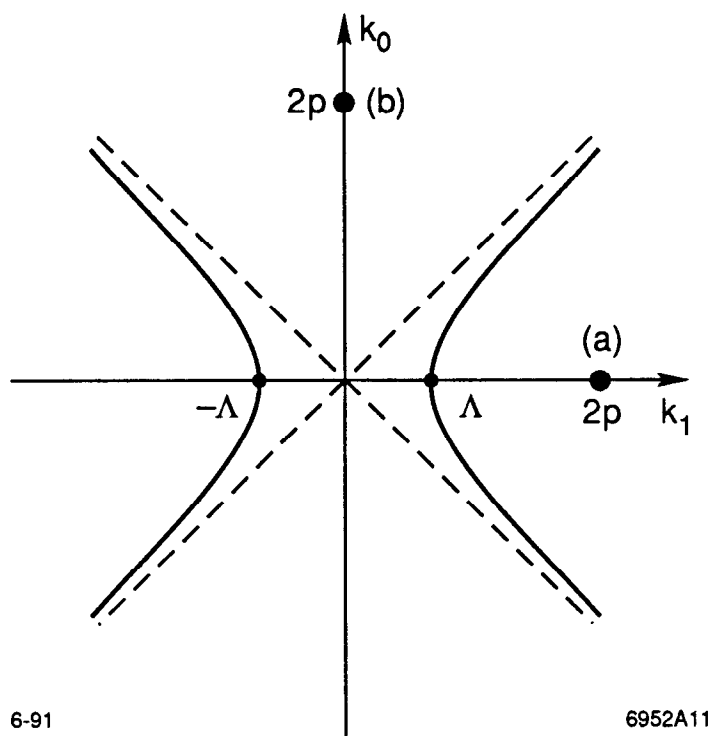


Fig 11

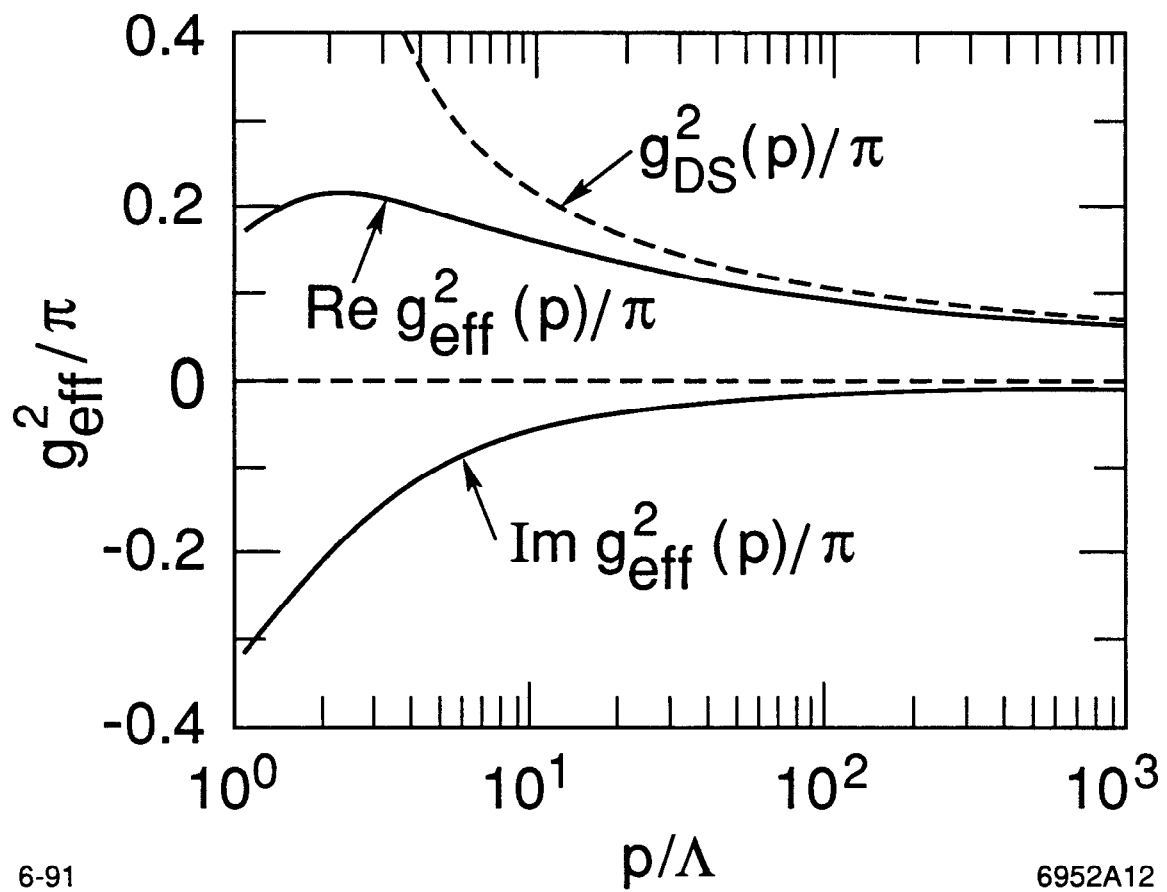
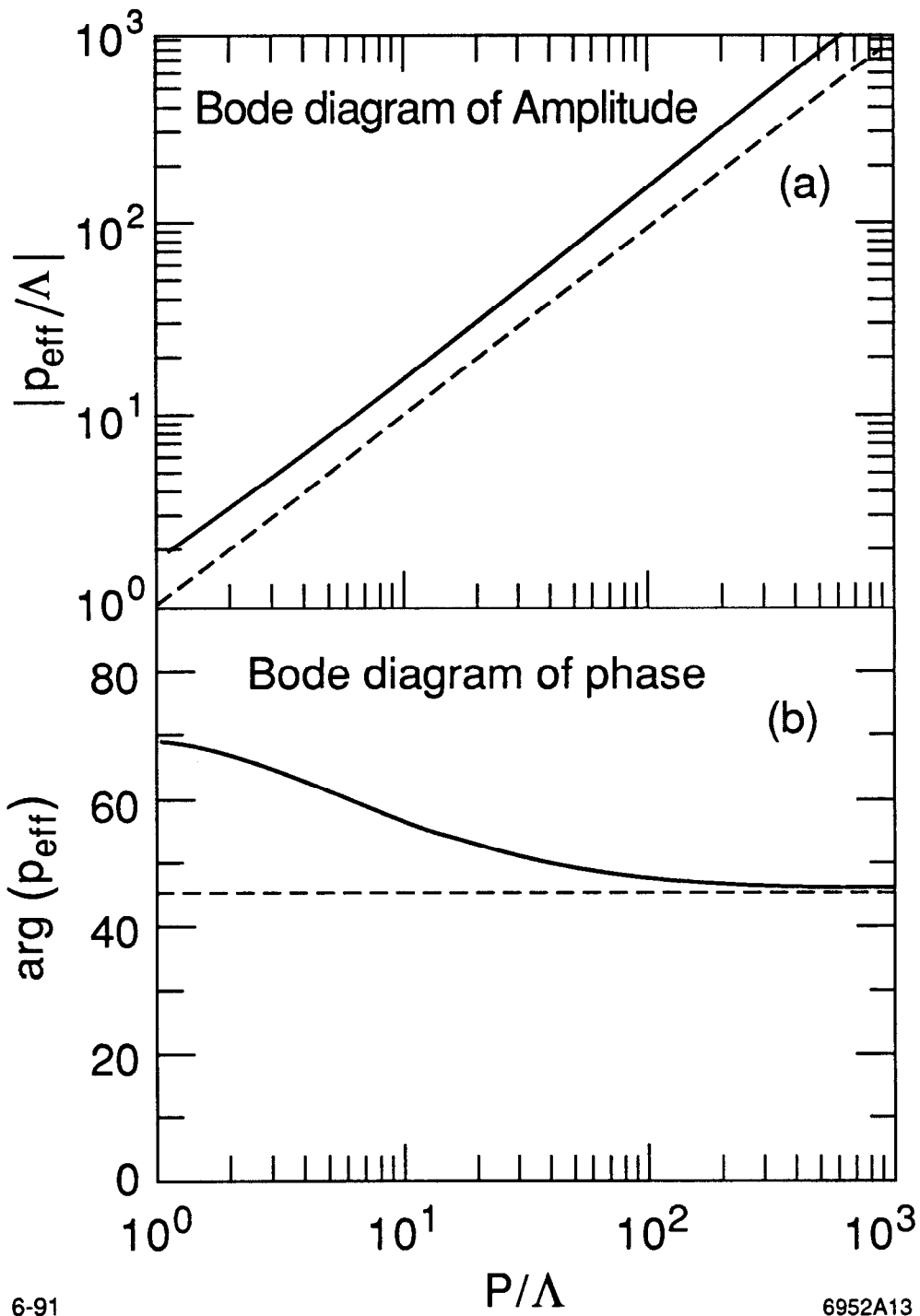


Fig 12



6-91

6952A13

Fig 13



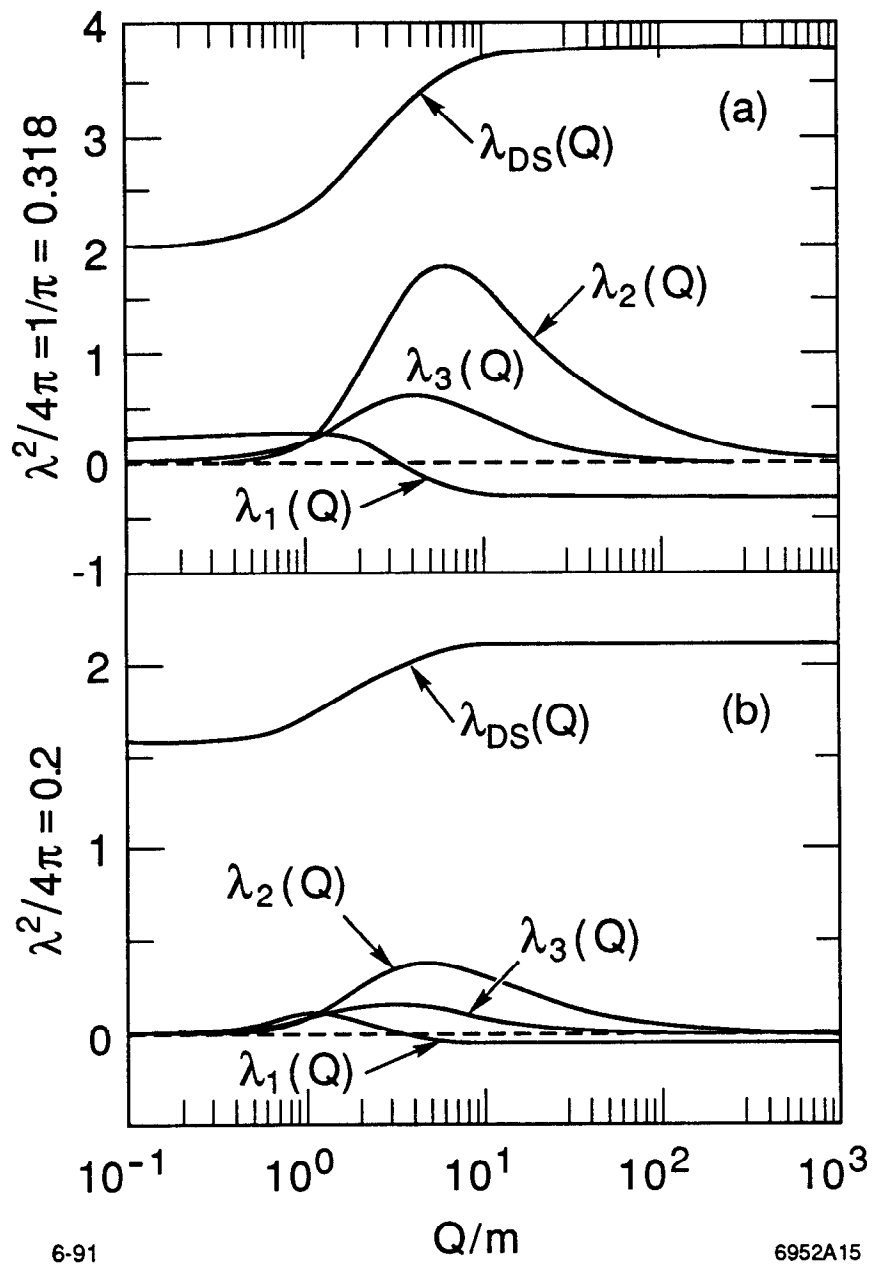
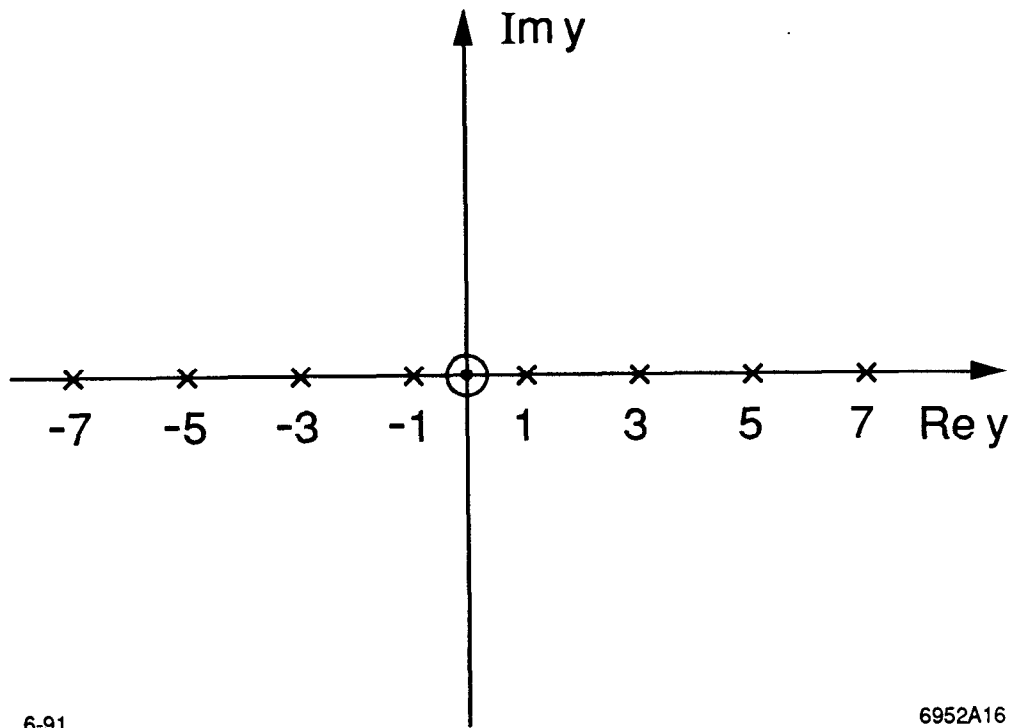


Fig 15



6-91

6952A16

Fig 16